Single-cell profiling of the microenvironment in decidual tissue from women with missed abortions

Ren Hou, M.D, Ph.D.,[a,b] Renliang Huang, M.M.,[a] Yanling Zhou, M.M.,[b] Dan Lin, B.S.,[a] Jing Xu, M.M.,[a] Liuqing Yang, B.S.,[a] Xiaolan Wei, M.M.,[c] Zhuoming Xie, M.S.,[c] and Qiaomiao Zhou, M.M.[a]

[a] Department of Genetics and Prenatal Diagnosis, Hainan Women and Children's Medical Center, Haikou, People's Republic of China; [b] Department of Eugenics and Genetics, The Affiliated Hospital of Guilin Medical University, Guangxi Zhuang Autonomous Region, People's Republic of China; and [c] Beijing SeekGene BioSciences, Beijing, People's Republic of China

Objective: To define the decidual microenvironment in euploid and aneuploid missed abortions and elective termination of pregnancies.
Design: Prospective, multicenter, observational study.
Setting: Tertiary hospital and descriptive analysis of transcriptomic data.
Patient(s): A total of 34 patients experienced abortions, including 6 women who underwent elective terminations of pregnancy of unplanned pregnancies and 28 cases with missed abortions. All patients underwent their operations from Sep, 2021 to Sep, 2022.
Intervention(s): All women underwent villous copy number variation sequencing. Meanwhile, single-cell RNA sequencing were performed in the decidual tissues of 16 women, and reverse transcription quantitative polymerase chain reaction were performed in the decidual tissues of 18 women.
Main Outcome Measure(s): Single-cell RNA sequencing was used to explore the changes in the microenvironment of decidual tissues in abortions.
Result(s): Single-cell RNA sequencing indicated that the microenvironment of the decidual tissue of the missed-abortion group was altered, and that the stromal cells (SCs), natural killer cells, macrophages, and epithelial cells all reflected functional imbalances compared with the elective terminations of pregnancy group. We also noted a correlation between the proportion of senescent SCs and chromosomal abnormalities in missed-abortion embryos. The proportion of senescent decidual SCs in the decidual tissue of missed-abortion patients with common chromosomal abnormalities of the fetus was higher, and this was not conducive to fetal growth and was closely related to missed abortion. In addition, we ascertained that the strength of the *HLA-KIR* interaction between NK1 and NK2 subsets and non-senescent stromal cell subsets in the missed abortion decidual tissues was weakened, potentially playing a role in the occurrence of missed abortion.
Conclusion(s): The decidualization of SCs in the missed-abortion decidual tissues was impaired, the clearance of senescent SCs by NK cells was weakened, the killing toxicity of non-senescent SCs was enhanced, macrophages were insufficiently resident at the maternal–fetal interface, and epithelial cell differentiation was unbalanced—all creating a maternal microenvironment that was not conducive to fetal growth. We posit that interfering with the expression of dysregulated genes in the missed-abortion decidual tissues and reversing the maternal microenvironment might constitute an effective means toward improving the clinical outcome of missed abortions. Intriguingly, we observed a correlation between stromal cell senescence and embryonic chromosomal abnormalities. Thus, we hypothesize that the *DIO2* marker of senescent SCs can be used as a risk indicator for the occurrence of missed miscarriages with chromosomal abnormalities of the embryos, and that it can be applied to guide the clinical diagnosis and treatment of recurrent abortion.
Clinical Trial Registration Number: NCT04425317. (Fertil Steril® 2023;119:492-503. ©2022 by American Society for Reproductive Medicine.)
El resumen está disponible en Español al final del artículo.

Key Words: Missed abortion, decidual stromal cells (DSCs), senescent stromal cells (snSCs), chromosomal aneuploidy, microenvironment

Received July 17, 2022; revised December 4, 2022; accepted December 7, 2022; published online December 15, 2022.
Supported by the Major Science and Technology Program of Hainan Province (Grant No.ZDKJ2021037), and the Project of Hainan Province Clinical Medical Center (QWYH202175).
R.H. has nothing to disclose. R.H. has nothing to disclose. Y.Z. has nothing to disclose. D.L. has nothing to disclose. J.X. has nothing to disclose. L.Y. has nothing to disclose. X.W. has nothing to disclose. Z.X. has nothing to disclose. Q.Z. reports grant from the Major Science and Technology Program of Hainan Province (grant No.ZDKJ2021037) , and the Project of Hainan Province Clinical Medical Center (QWYH202175).
R.H. and R.H. should be considered similar in author order.
Correspondence to: Qiaomiao Zhou, M.M., Department of Genetics and Prenatal Diagnosis, Hainan Women and Children's Medical Center, Haikou, People's Republic of China (E-mail: zhouqiaomiao@126.com).

Fertility and Sterility® Vol. 119, No. 3, March 2023 0015-0282

https://doi.org/10.1016/j.fertnstert.2022.12.016

Nearly 15% of pregnancies end in abortion (1), generally in the first trimester. Early missed abortion refers to death of the embryo or fetus before 12 weeks of gestation, with the conceptus fragments remaining in the uterine cavity without timely extrusion. Missed abortions beset patients and families with serious psychological burdens, but the mechanism(s) leading to such abortions remains to be elucidated. It is currently posited that 56%–60% of miscarriages are due to fetal chromosomal abnormalities (2) that relate to maternal immune abnormalities, thrombophilia, infection, uterine mechanical damage, morphological abnormalities, and abnormal hormonal and endocrine levels (3). With each additional abortion, the likelihood of a subsequent successful pregnancy diminishes (1). However, many of the couples who miscarried due to fetal chromosomal abnormalities were themselves chromosomally normal and of the appropriate chronological age so as to be able to conceive healthy embryos after experiencing one or more spontaneous miscarriages. Whether a chromosomal anomaly-related missed miscarriage is an accidental phenomenon that occurs during embryonic development or whether there are risk factors involved in its occurrence is currently unclear. It is therefore important to improve the overall reproductive success rate by exploring the changes in the decidual microenvironment in missed abortions, to assess their relation to embryonic chromosomal abnormalities, as well as to diagnose and treat the condition.

The maternal–fetal interface is principally composed of embryonic trophoblast cells, maternal decidual stromal cells (DSCs), and various immune cells such as decidual natural killer (dNK) cells, macrophages (Mϕ), dendritic cells (DCs), T cells, B cells, and NKT cells as well as the soluble factors derived from these cells (4). Different subgroups of cells display different functions, but the specific subgroups that contribute to the occurrence of miscarriage remain unclear and require further clarification. Cells act as an independent functional unit, and disparate cells occupy different roles. In addition, dNK cells are the most abundant immune cell population at the maternal–fetal interface, and are primarily responsible for developing immune tolerance to the fetus, promoting extravillous trophoblast (EVT) cell invasion, and remodeling of the uterine spiral arteries by interacting with EVT cells at the maternal–fetal interface (5).

Furthermore, the DSCs possess multiple biologic functions, including providing nutrients required for embryonic development, expressing receptors for pregnancy-related hormones under their control, secreting cytokines and chemokines specific to the maternal–fetal interface, and regulating the invasive behavior of the trophoblast; collectively, then, trophoblasts induce maternal–fetal immune balance and are critical to pregnancy maintenance. The physical and molecular interaction of the embryonic trophectoderm and the uterine epithelium allow the underlying stromal cells (SCs) to continue to differentiate (decidualization), but whether this decidualization of endometrial stromal cells (EnSCs) during embryonic implantation proceeds normally or becomes an early missed miscarriage is closely related to the overall sequence of abortion events (6). Studies have shown an increase in the senescent decidual cells (snDCs) in preterm women (7), suggesting that decidual senescence is important in preterm birth. Cellular senescence is a state comprising an essentially irreversible proliferative arrest combined with pronounced secretory activity. It includes the actions of various types of reactive oxygen species, extracellular matrix-remodeling proteins, proinflammatory cytokines, chemokines, and growth factors. The significant secretion of bioactive molecules thus generates the senescence-associated secretory phenotype (8). Age-related stimuli are more commonly found in genomic instability, telomere attrition, epigenetic alterations, loss of proteostasis, deregulated nutrient sensing, mitochondrial dysfunction, cellular senescence, stem cell exhaustion, and altered intercellular communication (9). Accumulation of snDCs leads to local enhancement of senescence-associated secretory phenotype, further stimulating augmented myometrial contractility, as well as membrane activation and attenuation, in the presence of proinflammatory cytokines.

Earlier detection technologies lacked the necessary depth, analysis rate, and accuracy in the study of missed abortion. Single-cell technology, in contrast, takes the basic functional unit of life, i.e., the cell, as the research object, and offers a higher resolution that allows the deeper exploration of various developmental states. The heterogeneity of the microenvironment in which the embryo thrives can be used to infer communication networks between different cell types at the maternal–fetal interface (10), thus providing a powerful means to uncover and analyze novel cellular subpopulations of highly heterogeneous cell populations (11). In the present study, we exploited single-cell RNA-seq to construct a single-cell map of the decidual tissue of induced and missed abortions, examined the microenvironment of decidual tissue of chromosomally aneuploid and chromosomally normal missed abortions and unplanned-pregnancy elective terminations of pregnancy, and further analyzed the mechanism(s) underlying missed abortions.

MATERIALS AND METHODS

Study ethics approval was granted by the institutional review board (No. HNWCMC202206).The data that support the findings of this study have been deposited into CNGB Sequence Archive (CNSA) of China National GeneBank DataBase (CNGBdb) with accession number CNP0003470 (12, 13).

Cell Preparation

The villi and decidua were selected from the patients who had missed abortions within 12 weeks of gestation, and the embryos had died and remained in the uterine cavity and could not be discharged spontaneously in time. All of them were obtained through elective terminations of pregnancy, excluding in vitro fertilization patients who experienced a spontaneous pregnancy loss after embryo transfer.

After harvesting, tissues were washed in ice-cold RPMI-1640 Medium (Hyclone, Catalog No. SH30809.01) and dissociated using a Multi-tissue Dissociation Kit 2 (Miltenyi Catalog No. 130-110-203) from Miltenyi Biotec according to the manufacturer's instructions. DNase treatment was used optionally in accordance with the viscosity of the

homogenate. We estimated cell counts and viability using a fluorescence cell analyzer (Countstar Rigel S2) with acridine orange/propidium iodide reagents after removing erythrocytes (Miltenyi, 130-094-183), and debris as well as dead cells were removed as needed (Miltenyi, 130-109-398/130-090-101). Finally, fresh cells were washed twice in RPMI-1640 and then resuspended at 1×10^6 cells per mL in 1×PBS and 0.04% bovine serum albumin.

Single-cell RNA-seq Library Construction and Sequencing

Single-cell RNA-seq libraries were prepared using a SeekOne MM Single Cell 3' Library Preparation Kit (SeekGene, Catalog No. K00104-04). Briefly, an appropriate number of cells were loaded into the flow channel of the SeekOne MM chip that had 170,000 microwells, and cells were allowed to settle in the microwells by gravity. After removing the nonsettled cells, sufficient cell barcoded magnetic beads (CBBs) were pipetted into the flow channel and also allowed to settle in the microwells under a magnetic field. Next, excess CBBs were rinsed out, and cells in the MM chip were lysed to release the RNA captured by the CBB in the same microwell. All CBBs were then collected, and reverse transcription was performed at 37 °C for 30 min to label the cDNA with the cell barcode on the beads, and exonuclease I treatment was applied to remove unused primer on the CBBs. Barcoded cDNA on the CBBs was subsequently hybridized with random primers that had a reads 2 SeqPrimer sequence at the 5' end and that could extend to form the second-strand DNA with the cell barcode at the 3' end. The resulting second-strand DNA was denatured off the CBBs, purified, and ultimately amplified in polymerase chain reaction (PCR) reaction. The amplified cDNA product was then cleaned to remove unwanted fragments and added to full-length sequencing adapters and sample index by indexed PCR. The indexed sequencing libraries were cleaned with solid phase reverse immobilization beads, quantified by quantitative PCR (KAPA Biosystems KK4824), and then sequenced on an Illumina NovaSeq 6000 machine with a PE150 read length.

Processing Single-cell RNA Sequencing Data

The raw sequencing data were processed first with Fastp (14) to trim the primer sequences and low-quality bases. We used SeekOneTools (Beijing SeekGene BioSciences) to process the sequencing data and align the sequences to human GRCh38 to obtain a gene-expression matrix. We used Seurat (4.0.3) to filter low- quality cells and cells with a number of detected genes at <200 or >6000; cells with a high percentage (20%–40%) of mitochondrial genes were also omitted. The remaining cells were then used for subsequent analysis.

Canonical Correlation Analysis, Dimensionality Reduction, and Clustering

After quality control and filtering, clustering and visualization were completed with Seurat (15) (V4.0.3) using the following steps. Library-size normalization to each cell was conducted by NormalizeData, the variable genes were calculated with FindVariableGenes, all libraries were combined using FindIntegrationAnchors and IntegrateData with default parameters, and ScaleData was employed to regress out the variability of the numbers of unique molecular identifiers. RunPCA and RunUMAP were implemented to reduce dimensions, and FindClusters was exploited to cluster the cells using 30 dims at a resolution of 0.6 (for a total of 25 clusters).

FindAllMarkers was applied to compare each cluster to all the others to identify cluster-specific marker genes. Each retained marker gene was then expressed in a minimum of 25% of cells and at a minimal log fold-change threshold of 0.25. The clustered differentially expressed genes (DEGs) were considered significant if the adjusted P value was <0.05 and the avg._log2FC was ≥ 0.

Stromal and NK cells were then allocated into respective subsets and further clustered into subclusters using the default parameters described above. According to published gene expression (16), SCs were clustered into 2 cell clusters, senescence (sn) and non-senescence (non-sn), and NK cells were clustered into NK1, NK2, and NK3 subsets.

Cell–cell Interactions

We used CellPhoneDB (10) to infer cell–cell interactions, and log-transformed and normalized counts and cell-type annotations were used as inputs. To narrow the most relevant interactions, we identified specific interactions classified by ligand and receptor expression in more than 10% of cells within a cluster and when $\log_2$ mean expression of the ligand and receptor pair was greater than 0.

Pseudotime Analysis

We applied Monocle software (version 2.3.6) (17) to determine the potential lineage differentiation between cellular populations using default parameters. CellDataSet object was created with recommended parameters, dispersion Table function was used to determine genes used for pseudotime ordering. The DDRTree method was utilized for dimension reduction and cell ordering along the pseudotime trajectory, and branch analysis (with branch point 1) was conducted using the branched expression analysis modeling function. The significantly changed genes in the branch point were clustered using plot_genes_branched_pseudotime functions according to the distinct patterns of gene-expression changes.

Enrichment Analysis

Gene Ontology–enrichment analysis of marker genes was implemented with the clusterProfiler R package, and Gene Ontology terms with a corrected P value <0.05 were considered significantly enriched by the marker gene.

Copy Number Variation Sequencing

Each fetal villus sample was used to extract genomic DNA, the obtained 300 ng genomic DNA was fragmentated and purified using the MagPur A3 XP Kit (Magen). After an end repair step, the sequencing adapter was ligated to the input DNA. To distinguish different libraries, index sequences were

introduced by a PCR step. In accordance with the manufacturer's instructions, DNA libraries were quantified and amplified by emulsion PCR, and the enriched particles were sequenced by the Daan gene DA8600 sequencer (DAAN GENE,Guangzhou, China). Clean data were obtained by removing read when the mapq was lower than 30 and mapped to the reference human genome version hg19. The bam file of each sample was analyzed by the copy number variation plug-in (Darui Biotechnology, Guangzhou, China)to obtain the copy number (CNs value), and the results were judged according to the reference range. The resolution was 100 kb with bin size of 50 kb. Approximately 3 million single end 100 bp reads were obtained for copy number variation analysis.

Reverse transcription quantitative PCR

Total RNA was extracted from decidual tissue, using RNAiso Plus (Takara, Shiga, Japan) according to the manufacturer's instructions. The Hifair II 1st Strand cDNA Synthesis Kit (Yeasen Biotechnology, Shanghai, China) was used with 1.5 μg of total RNA in 20 μL reactions. Amplification was performed on a ViiA 7 Real-Time PCR system (Applied Biosystems, Paisley, UK) in 10 μL reactions using 2×ChamQ Universal SYBR qPCR Master Mix (Vazyme Biotech, Nanjing, China), with 200 nM each of forward and reverse primers. Reference control is *RPL19*. The primer sequences were as follows: *SCARA5* forward: 5′-CCT GTC CAA GCT GAA CCT GT-3′, *SCARA5* reverse: 5′-GGC CTG GAC ACT GCT AAG AT-3′; *DIO2* forward: 5′-CCT CAG TGG CTG ACT TCC TG-3′, *DIO2* reverse: 5′-GCA AGG AGA AAC GCT CCA GA-3′, *RPL19* forward: 5′-CAA CTC CCG TCA GCA GAT CC-3′, *RPL19* reverse: 5′-CCC TTC CGC TTA CCT ATG CC-3′. The ΔCt is calculated by normalizing the Ct of the target sample with the Ct of the endogenous control and relative abundances = *DIO2* POWER(2, ΔCt) / *SCARA5* POWER(2, ΔCt).

Statistical Analysis

Spearman's correlation analysis was conducted to explore the correlation between the percentage of senescent SCs per sample and other variables. We calculated Spearman's coefficient, using a two-sided *P* value of <0.05 as statistically significant. The Wilcoxon's rank sum test was also applied to evaluate the expression differences in selected genes between the sample groups. All statistical analyses were performed using R (version 3.6.1).

RESULTS

Single-cell Mapping of Decidua in Missed and Normal Abortions

To investigate whether the changes in the decidual microenvironment were related to fetal chromosomal abnormalities, we collected the decidual and fetal villous tissues from 16 women who aborted in the first trimester, including 2 cases of elective terminations of pregnancy (the NC group) and 14 cases of missed abortions (the MA group). The decidual tissue was subjected to single-cell RNA sequencing, and fetal villous tissue was subjected to copy number variation sequencing. The MA group was further subclassified according to the presence of chromosomal abnormalities in the fetus, including 12 cases with fetal chromosomal aneuploidy (MA-A group) and 2 cases with normal fetal chromosomes (MA-N group) (Fig. 1A) (Supplemental Table 1, available online). After quality filtering and batch correction, graph-based clustering was performed to group a total of 102,787 cells according to gene-expression profiles (Fig. 1B). There were 9 major clusters in both NC group and MA group samples, including NK cells, monocytes, epithelial cells, SCs, DCs, endothelial cells, Mϕ, neutrophils, and B cells (Fig. 1C). NK cells accounted for the largest proportion of immune cells in the majority of decidual tissues, whereas neutrophils accounted for the highest proportion in PL001, PL012, and PL013 samples (Fig. 1D); the granulocyte index was normal (Supplemental Table 1). Compared with the NC group, the proportion of SCs decreased and the proportion of immune-related cells increased in the MA group (Fig. 1D).

Characteristics of Decidual NK Cells

By analyzing the DEGs between MA and NC groups, we found that decidual NK cells in the MA group were significantly up-regulated in their expression of a group of heat-shock protein 70 genes (*HSPA1A*, *HSPA6,* and *HSPA1B*) and down-regulated the expression of *GNLY*, *KIR2DL1,* and *KIR2DL3* (Fig. 2A) (Supplemental Table 2, available online). In addition, the significantly up-regulated DEGs in the MA group were principally enriched in heat-shock protein binding, response to heat stress, and exogenous apoptosis-related signaling pathways (Fig. 2B) (Supplemental Table 2). When we subclustered the NK cells we obtained 4 subpopulations (NK1, NK2, NK3, and undefined) by co-annotation of marker genes (Fig. 2C–2D). Analysis of DEGs revealed that the NK1 and NK2 subsets (hereinafter collectively referred to as NK1_2) showed a higher expression of *KIR2DL1*, *KIR2DL3*, *KIR2DL4,* and *NCAM1* relative to NK3 (Fig. 2E and Supplemental Table 2). Analysis of receptor–ligand interactions found that there were interactions with *HLA-C_KIR2DL1* and *HLA-C_KIR2DL3* between SCs and NK1_2 in the NC group, but the interactions were not observed in the MA group (Fig. 2F). The functionality of decidual NK cells in the missed-abortion group was altered relative to that in the NC group, and the maternal environment may not be conducive to the growth and development of the fetus.

Characteristics of DSCs

The differentiation and transformation of EnSCs into specialized DSCs before and during pregnancy is one of the foundations for the initiation and maintenance of pregnancy. Therefore, we analyzed the SCs in the decidua between the MA and NC groups and found that the DEGs in the MA group exhibited significantly down-regulated OSR2, growth factor-related genes, *MMP19* and *HAND2*, as well as also showed up-regulated *SERPINE2*, *MMP10*, *TIMP3,* and collagen-related genes (Fig. 3A and Supplemental Table 2).

After subclustering of SCs, 2 subpopulations of senescent stromal cells (snSCs) and non-snSCs were obtained using senescence-related marker gene annotation (Fig. 3B–3C).

FIGURE 1

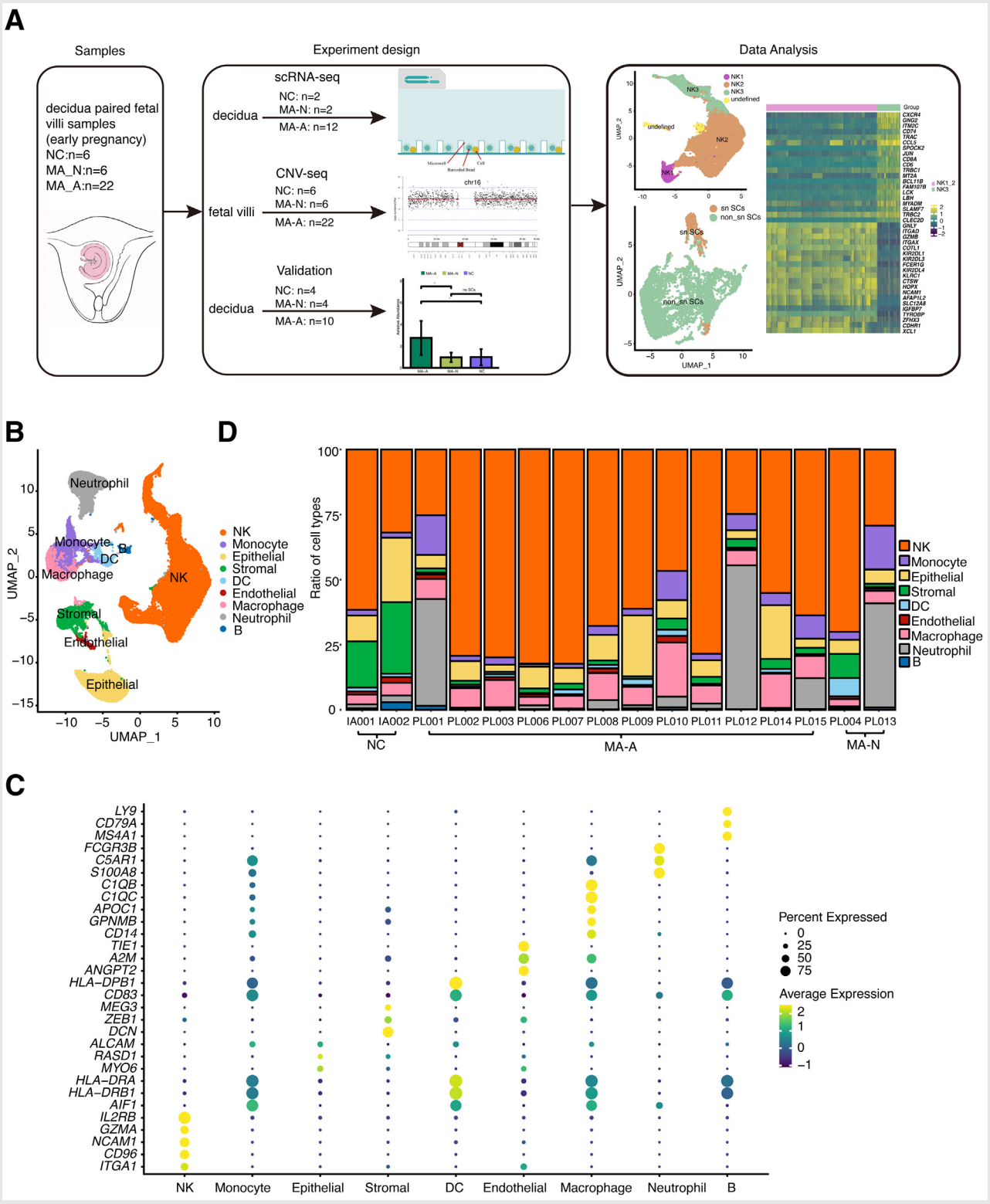

(A) Schematic overview. (B) Umap representation for cell type. Color-coded for cell type. (C) Dot plot representing average expression (dot color) and percent expression (dot size) of markers defining all cell types. (D) Fraction of cells in each cell type per sample.

Hou. Single-cell profiling of missed abortions. Fertil Steril 2023.

FIGURE 2

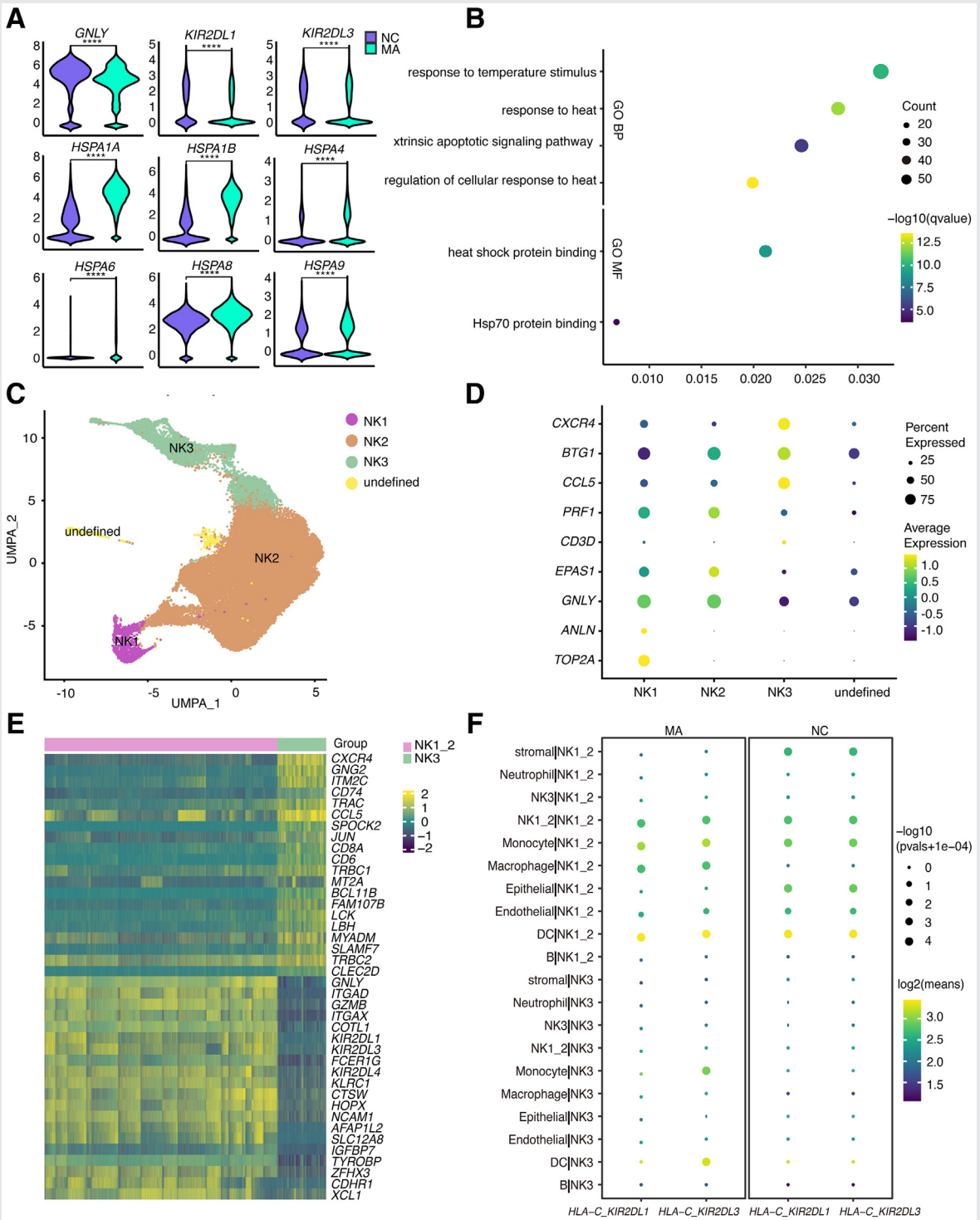

(A) Violin plots representing expression profiles of NK cells between MA and NC; ****$P \leq 0.0001$. (B) Dot plot representing P value (dot color) and gene ratio (dot size) of enrichment terms based on differentially expressed genes in NK cells between MA and NC. (C) Umap representation for all NK subtypes. Color-coded for subtypes. (D) Dot plot representing average expression (dot color) and percent expression (dot size) of markers defining all NK subtypes. (E) Heatmap of differentially expressed genes in all NK subtypes. (F) Dot plot representing selected ligand–receptor interactions per cell type in all sample groups, P values indicated by circle size, scale on right. The means of the average expression level of interacting molecule 1 in cell type 1 and interacting molecule 2 in cell type 2 are indicated by color. Interacting molecules and cell types are divided by underline and vertical line separately.

Hou. Single-cell profiling of missed abortions. Fertil Steril 2023.

FIGURE 3

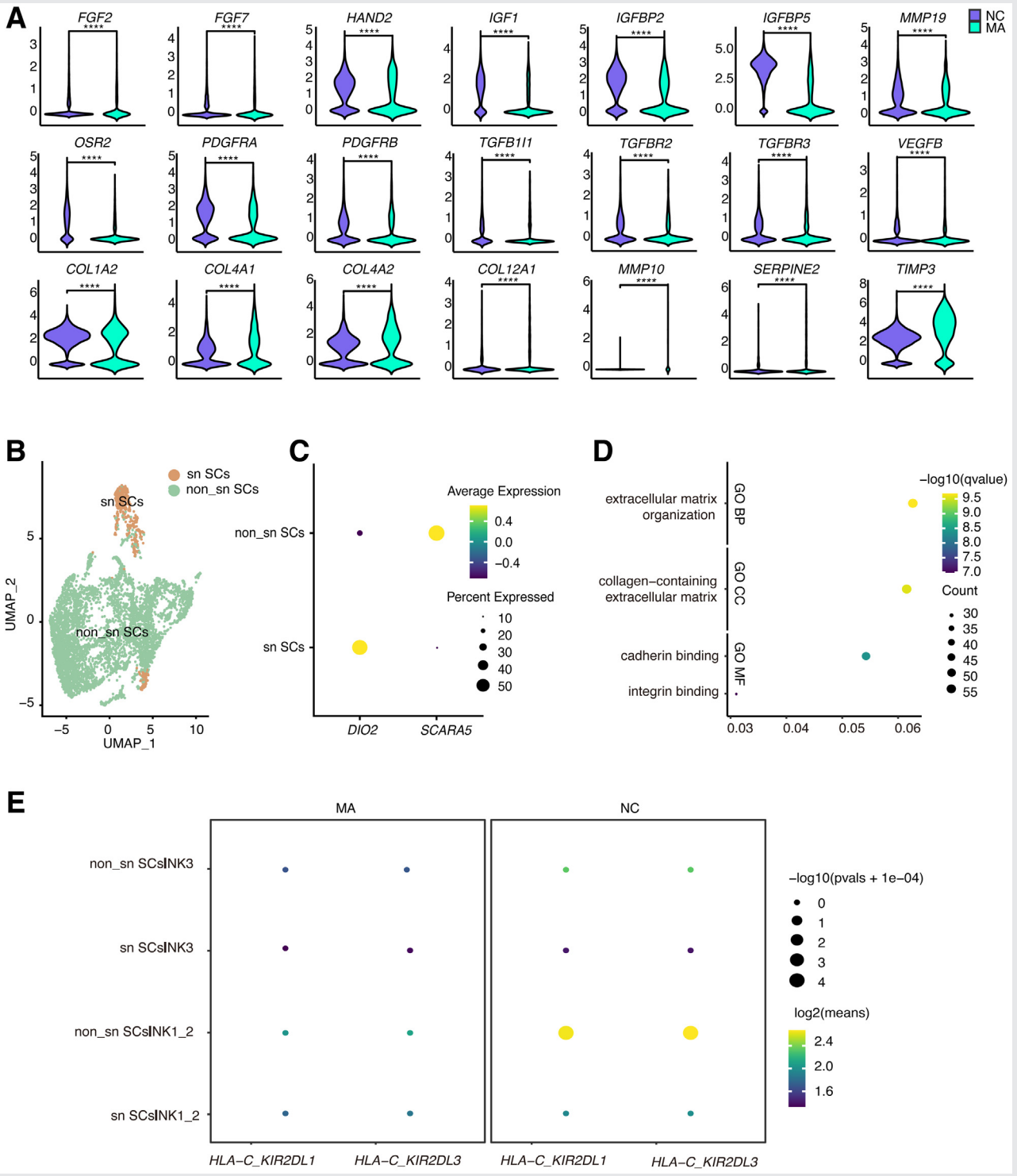

(A) Violin plots representing expression profiles of SCs between MA and NC; ****$P \leq 0.0001$. (B) Umap representation for sn and non_sn SCs subtypes. Color-coded for subtypes. (C) Dot plot representing average expression (dot color) and percent expression (dot size) of markers defining all SCs subtypes. (D) Dot plot representing *P* value (dot color) and gene ratio (dot size) of enrichment terms based on differentially expressed genes in non-snSCs between MA and NC. e Dot plot representing selected ligand–receptor interactions per cell type in all sample groups, *P* values indicated by circle size, scale on right. The means of the average expression level of interacting molecule 1 in cell type 1 and interacting molecule 2 in cell type 2 are indicated by color. Interacting molecules and cell types are divided by underline and vertical line separately.

Hou. Single-cell profiling of missed abortions. Fertil Steril 2023.

FIGURE 4

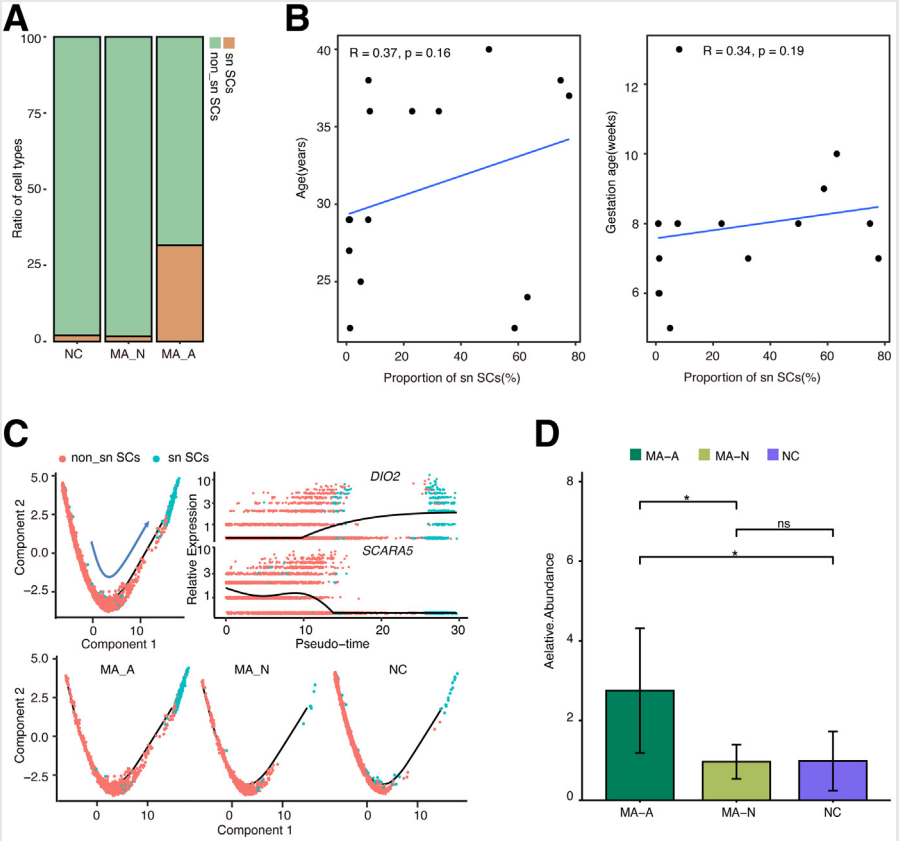

(A) Fraction of cells in each SCs subtype per sample group. (B) Spearman's correlation analysis between proportion of snSCs and baseline information (age and gestation age). (C) Lineage differentiation trajectory of SCs. Relative expression of marker genes, by state, is shown at the top right side of the figure. (D) The relative abundace analysis of *DIO2* / *SCARA5* in NC, MA-N and MA-A group; *$P<0.05$. ns: no significant.

Hou. Single-cell profiling of missed abortions. Fertil Steril 2023.

With regard to non-snSCs, the MA group comprised significantly up-regulated DEGs enriched in extracellular matrix binding-related signaling pathways compared with the NC group (Fig. 3D, Table S2). In the analysis of NK cell characteristics we determined that the SCs in the NC group interacted with the NK1_2 cell subsets, and we then further analyzed the cellular communication between the SCs subsets and the NK cell subsets in the NC and MA group. We noted that only the *HLA-C-KIR2DL1* and *HLA-C-KIR2DL3* interacted between non-snSCs and NK1_2 cells in the NC group (Fig. 3E).

In addition, we observed that the proportion of snSCs in the MA-A group was significantly higher than that in the NC and MA-N groups, and that the distributional difference was not correlated with pregnant age and gestational age (Fig. 4A and 4B). Because we also noted that the proportions of snSC in the NC and MA-N groups were less than 10%, we then divided samples in the MA-A group into 2 subgroups by taking the proportion of snSCs at the cut-off value of 10%. A clinical comparison of the 2 subgroups showed that the fetal aneuploid abnormalities in the high-proportion group were more common (Table S3).Pseudotime analysis was conducted on the SCs of the 3 groups, and we determined that the differentiative trend in SCs was the same among the 3 groups, although there were differences in the distribution of snSCs and non-snSCs among the groups (Fig. 4C). In the process of differentiation from non-snSCs to snSCs, the expression of *DIO2* gradually increases, and the expression of *SCARA5* gradually decreases (Fig. 4C).Real-time PCR was performed to further analyze the relative abundance of *DIO2* / *SCARA5* among NC, MA-N and MA-A group. The relative abundance of *DIO2* / *SCARA5* was significantly high in the MA-A group than NC and MA-N group ($P<0.05$) (Fig. 4C). The fetal aneuploid abnormalities in the high relative abundance (*DIO2*/*SCARA5*>2) samples of MA-A group were more common in clinical medicine.

Characterization of Decidual Macrophages

Massively infiltrating and enriched decidual macrophages (dMϕ), which are widely recognized as important regulators of maternal–fetal immunotolerance and trophoblast invasion, contribute to normal pregnancy. Analysis of DEGs in Mϕ between the MA and NC groups showed that in the MA group the autophagy gene *ATG* was up-regulated, whereas

we observed down-regulation of *LPAR6* and genes related to the pro-angiogenic factors *IGFBP4*, *IGFBP7,* and *IGF1* (Supplemental Fig. 1A, available online) (Supplemental Table 2). The differential gene-enriched signaling pathways that were down-regulated in the MA group compared with the NC group involved negative regulation of cell migration, cell adhesion, and growth factors (Supplemental Fig. 1B, available online) (Supplemental Table 2). The inactivation of lysophosphatidic acid metabolism and autophagy of dMϕ in the MA group thus led to insufficient residence at the maternal–fetal interface, which affected the immune microenvironment balance at the maternal–fetal interface.

Characteristic of Decidual Epithelial Cells

We next analyzed the DEGs of epithelial cells in the decidual tissue in the MA and NC groups, and found down-regulation of the Wnt-signaling pathway-related gene *JUN* in the NC group, and up-regulation of the Notch signaling pathway-related genes *ANXA4*, *MDK*, *YBX1,* and *IL6ST*; the secretory epithelial cell marker gene *DEFB1*; and transcription factors related to Wnt-signaling pathway inhibition (*HNF1B*, *FOXO1*, and *HIF1A*) (Supplemental Fig. 2, available online) (Supplemental Table 2). The imbalance between Wnt and Notch pathway regulation in the differentiation of epithelial cells in decidual tissue from missed abortions thus affected the maternal decidual microenvironment and may be not conducive to fetal survival.

DISCUSSION

With the increasing awareness of developmental abnormalities at the maternal–fetal interface during pregnancy and preterm birth, more attention has been given to the relationship between adverse embryonic development in early pregnancy and the decidua. Although SCs support normal growth and development of the embryos after sufficient decidualization, the ability of decidualization to occur smoothly during embryonic implantation is key to the normal progression of pregnancy. Mature DSCs possess tight connections with other immune cells, and successful endometrial transformation in early pregnancy requires successful differentiation of the EnSCs into DSCs and the rapid elimination of snSCs by activated dNK cells; in contradistinction, the presence of defective snSCs within this process leads to early pregnancy loss (18). We herein constructed a single-cell atlas of decidual tissue from induced and missed abortions using single-cell RNA-seq, and demonstrated that the cell types annotated as NK, neutrophils, B, SCs, Mϕ, monocytes, SCs, epithelial cells, and endothelial cells were distributed within each sample. Except for SCs, the proportions of NK cells, monocytes, Mϕ, neutrophils, and other immune cells were higher in the missed-abortion decidual tissues than in the decidual tissue of the elective terminations of pregnancy group—indicating that the decidual tissue of the missed-abortion group possessed a higher proportion of immune cells, thereby reflecting an inflammatory microenvironment.

The dNK cell is the principal immune cell resident at the maternal–fetal interface (10). In our study, we analyzed the DEGs between the MA group and the NC group and found that the decidual NK cells in the MA group significantly up-regulated the expression of a group of heat-shock protein 70 genes; down-regulated the expression of *GNLY*, *KIR2DL1*, and *KIR2DL3* (19). *KIR* gene family and *GNLY* gene expression can enhance the killing ability to fetal bacterial infection and reduce the killing toxicity to fetal trophoblast (20), indicating that different types of NK cells play a role in the MA combined NC group.

In a study of NK cells from decidual samples of patients with recurrent abortions, investigators found the cells to be functionally divided into 2 groups: one that secretes growth factors and supports embryonic growth, and the other that secretes cytokines that promote the formation of an inflammatory environment in the decidua and that are detrimental to embryonic growth; a lack of protective NK cells then leads to recurrent miscarriages (21). We identified 3 major dNK cell subsets (NK1, NK2, and NK3) by single-cell RNA-seq, of which NK1 and NK2 exhibited similar gene-expression profiles, with a higher expression of genes encoding *KIR* proteins and *NCAM1* relative to NK3. Studies have shown that the expression of the *KIR* gene family not only inhibits the maternal attack on the fetus, but that *NCAM1*+ NK cells can eliminate decidualized snSCs, maintain endometrial homeostasis, and successfully complete decidualization (18). We observed that NK1/2 subsets functionally inhibited cytotoxicity toward embryos and removed snSCs, exerting a protective effect on embryonic development, whereas NK3 subtypes manifested no obvious role in the transformation of senescent cells and reduced the maternal effect on the fetus. Thus, NK cells exerted both protective and lethal actions on embryonic development, depending on the cell subtype (16). Analysis of cellular communication between different NK subsets and other cell types revealed that NK1/2 in the MA group attenuated the strength of the *HLA-KIR* interaction with SCs compared with the NC group, and that the NK1/2 subsets in missed abortions were more toxic to maternal stromal cells than in the NC group. When we further evaluated the cellular communication between NK subsets and stromal cell subsets, we demonstrated that the NK1/2 cells in MA group down-regulated the robustness of the *HLA-KIR* interaction with non-snSCs compared with the NC group. Compared with the NC, the NK1/2 subset in the MA group manifested dysfunctional actions that not only enhanced cytotoxicity to non-snSCs but also weakened the scavenging activity of senescent SCs, disrupting the balance of the maternal microenvironment.

This study was the first to depict a correlation between the proportion of decidual snSCs in missed abortions and embryonic chromosomal anomalies, potentially affecting the maternal decidual microenvironment and causing missed abortions. After subgrouping the collected samples according to the snSC maker *DIO2* and non-snSC maker *SCARA5*, we demonstrated that snSCs up-regulated differential genes enriched in multiple signaling pathways involved in cell adhesion, creating difficulty in clearing snSCs. Increased sn abundance was reported to create a maternal environment in which inflammation exacerbated progesterone resistance and was detrimental to fetal development (16). Although the differentiative trend in SCs was consistent among the 3

groups in the present study, we noted differences in the distributions of senescent and non-senescent SCs among the groups, with a significantly greater proportion of snSCs in the group of aborted embryos with chromosomal abnormalities than in the other 2 groups. Only a small fraction of the NC group differentiated into senescent SCs.

Earlier studies showed that senescence occurred during mouse development (22), and that cellular senescence was a process within embryonic development. Because the abnormal chromosomal condition of tetraploidy can be found in the EVTs of hyperplastic complete moles, tetraploidy is posited to trigger cellular senescence as a process limiting doubling during the placental development to prevent excessive polyploidization, genomic instability, and tumorigenesis (23). It was also reported that different levels of embryo-derived substances secreted by embryos of disparate quality appeared to determine the activity of dNK cells—particularly in embryos with chromosomal abnormalities—with the killing activity of dNK toward snSCs being reduced (24). It is hypothesized that the senescence of DSCs is related to fetal chromosomal abnormality and fetal arrest. In patients with missed abortion, the incidence of chromosomal abnormalities in embryonic villi was approximately 29%–50%, and approximately 90% of embryonic chromosomal abnormalities were abnormal in their number of chromosomes, with autosomal trisomy the most common (including trisomies 13, 15, 16, 18, 22, and 21) (25). In monosomic abortion, euchromatids are relatively rare, and most are X chromatids that appear due to the loss of the X chromosome in couples. Despite the small sample size of the present study, the occurrence of chromosomes in commonly aborted embryos uncovered in our study was similar to that of previous studies. Intriguingly, we also found that among the DSCs of these embryos containing common abnormal chromosomes (e.g., 22, 16, 15, and X), senescent DSCs accounted for an elevated proportion, whereas senescent DSCs were found in less-frequent chromosomal trisomies (i.e., 10, 11, and 7) in embryos; for embryonic DCs without chromosomal aberrations, the proportion of senescent DSCs was low. Because these chromosomes commonly found in aborted tissues are primarily short- and medium-sized acrocentric chromosomes (except for sex-chromosome monosomy), the crossover process during the pachytene stage and the segregation stage process during diplotene stage may put these particular chromosomes at risk (26). Moreover, the biologic mechanisms controlling this process now appear to be susceptible to the senescent process. Based on single-cell transcriptomics analysis, we herein propose that fetal chromosomal abnormalities are related to the distributional abundances of SC subsets, and that their presence exacerbates the process of non-snSCs that differentiate into snSCs to form a maternal environment unfavorable for fetal growth. We therefore speculate that the snSC maker *DIO2* may serve as a viable risk indicator.

Decidual Mϕ plays a crucial role in apoptosis and cell clearance during pregnancy, and rapid and efficient removal of apoptotic cells prevents self-antigen leakage and inflammation. It plays a significant role in angiogenesis and spiral artery remodeling during the first trimester of pregnancy (27), as well as contributes to normal pregnancy. Analysis of DEGs in Mϕ between MA group and NC group showed that MA group up-regulated autophagy gene *ATG3* in Mϕ; down-regulated ENPP2-lysophosphatidic acid (LPA) receptor (*LPAR6* and angiogenic factor-related genes (*IGFBP4*, *IGFBP7*, *IGF1*). This may lead to an increase in Mϕ autophagy, which leads to a decrease in Mϕ. At the same time, activation of LPA not only promoted the adhesion and retention of dMϕ, but also promoted M2 differentiation during normal pregnancy. ENPP2-LPA metabolic inactivation and dMϕ resident impairment of autophagy leading to dMϕ also increases the risk of miscarriage (28). In the MA group, the normal balance of the immune microenvironment at the maternal–fetal interface was disrupted, resulting in missed miscarriages.

Endometrial epithelial cells consist of secretory epithelial cells and ciliated epithelial cells, which in normal decidual tissue exhibit a secretory cell profile (29). It has been reported that down-regulation of Wnt and Notch pathways in endometrial organoids increases the differentiation efficiency of secretory epithelial cells and ciliated epithelial cells, respectively, and found that the Notch pathway-induced secretory epithelium dominates in decidual tissue (30). Notch signaling pathway regulates cell proliferation, differentiation, and apoptosis (31), but in the decidua of the MA group, Notch pathway-related genes, secretory epithelial cell marker gene *DEFB1*, and transcription factors related to Wnt-signaling pathway inhibition were found to be down-regulated. This reduces the differentiation of secretory epithelium, which affects the maternal decidual environment and normal embryonic development.

There were some limitations to the present study. Owing to our small sample size, although we discerned a correlation between SCs and chromosomal abnormalities, we could not elucidate a causal relationship. In the future it will be necessary to further clarify the abortive mechanism(s) underlying chromosomally abnormal embryos and the relationship between stromal cell senescence and chromosomal abnormalities. The proportion of neutrophils in some decidual samples was very high, and the mechanism(s) governing its development remains to be determined.

In conclusion, we observed that stromal cell decidualization was impaired in the missed-abortion decidual tissues, NK cell clearance of snSCs was diminished, cytotoxicity against non-snSCs was enhanced, Mϕ were insufficiently resident at the maternal–fetal interface, and epithelial cell differentiation was unbalanced. These phenomena thus created a maternal microenvironment that was unfavorable for fetal growth. We posit that interfering with the expression of dysregulated genes in the missed-abortion decidual tissues and reversing an unhealthy maternal microenvironment may be an effective means toward improving the clinical outcome of missed abortions. We also noted a correlation between stromal cell senescence and embryonic chromosomal abnormalities. Therefore, *DIO2* as a marker of snSCs may be exploited as one of risk indicators for missed abortions in which the embryos exhibit chromosomal abnormalities, and *DIO2* may be helpful to guide the clinical diagnosis and treatment of recurrent abortion.

REFERENCES

1. Quenby S, Gallos ID, Dhillon-Smith RK, Podesek M, Stephenson MD, Fisher J, et al. Miscarriage matters: the epidemiological, physical, psychological, and economic costs of early pregnancy loss. Lancet 2021;397:1658–67.
2. Hardy K, Hardy PJ, Jacobs PA, Lewallen K, Hassold TJ. Temporal changes in chromosome abnormalities in human spontaneous abortions: results of 40 years of analysis. Am J Med Genet 2016;170:2671–80.
3. Arias-Sosa LA, Acosta ID, Lucena-Quevedo E, Moreno-Ortiz H, Esteban-Pérez C, Forero-Castro M. Genetic and epigenetic variations associated with idiopathic recurrent pregnancy loss. J Assist Reprod Genet 2018;35:355–66.
4. Xu YY, Wang SC, Li DJ, Du MR. Co-Signaling molecules in maternal–fetal immunity. Trends Mol Med 2017;23:46–58.
5. Knöfler M, Haider S, Saleh L, Pollheimer J, Gamage TKJB, James J. Human placenta and trophoblast development: key molecular mechanisms and model systems. Cell Mol Life Sci 2019;76:3479–96.
6. Ochoa-Bernal MA, Fazleabas AT. Physiologic events of embryo implantation and decidualization in human and non-human primates. Int J Mol Sci 2020;21:1973.
7. Feng L, Allen TK, Marinello WP, Murtha AP. Roles of progesterone receptor membrane component 1 in oxidative stress-induced aging in chorion cells. Reprod Sci 2019;26:394–403.
8. Tsuru A, Yoshie M, Kojima J, Yonekawa R, Azumi M, Kusama K, et al. PGRMC1 regulates cellular senescence via modulating FOXO1 expression in decidualizing endometrial stromal cells. Biomolecules 2022;12(8):1046.
9. Sanese P, Forte G, Disciglio V, Grossi V, Simone C. FOXO3 on the road to longevity: lessons from SNPs and chromatin hubs. Comput Struct Biotechnol J 2019;17:737–45.
10. Vento-Tormo R, Efremova M, Botting RA, Turco MY, Vento-Tormo M, Meyer KB, et al. Single-cell reconstruction of the early maternal–fetal interface in humans. Nature 2018;563:347–53.
11. Kiselev VY, Andrews TS, Hemberg M. Challenges in unsupervised clustering of single-cell RNA-seq data. Nat Rev Genet 2019;20:273–82.
12. Guo X, Chen F, Gao F, Li L, Liu K, You L, et al. CNSA: a data repository for archiving omics data (Oxford) 2020;2020:baaa055.
13. Chen FZ, You LJ, Yang F, Wang LN, Guo XQ, Gao F, et al. CNGBdb: China National GeneBank DataBase. Yi Chuan 2020;42:799–809.
14. Chen S, Zhou Y, Chen Y, Gu J. fastp: an ultra-fast all-in-one FASTQ preprocessor. Bioinformatics 2018;34:i884–90.
15. Butler A, Hoffman P, Smibert P, Papalexi E, Satija R. Integrating single-cell transcriptomic data across different conditions, technologies, and species. Nat Biotechnol 2018;36:411–20.
16. Lucas ES, Vrljicak P, Muter J, Diniz-da-Costa MM, Brighton PJ, Kong CS, et al. Recurrent pregnancy loss is associated with a pro-senescent decidual response during the peri-implantation window. Commun Biol 2020;3:37.
17. Trapnell C, Cacchiarelli D, Grimsby J, Pokharel P, Li S, Morse M, et al. The dynamics and regulators of cell fate decisions are revealed by pseudotemporal ordering of single cells. Nat Biotechnol 2014;32:381–6.
18. Brighton PJ, Maruyama Y, Fishwick K, Vrljicak P, Tewary S, Fujihara R, et al. Clearance of senescent decidual cells by uterine natural killer cells in cycling human endometrium. eLife 2017;6:e31274.
19. Peng YB, Liu H, Huang SH, Lai H, Zhou Q, Luo Y, et al. The study of the relationship between aberrant expression of hot shock protein 70 (HSP70) and spontaneous abortion. Eur Rev Med Pharmacol Sci 2017;21:652–6.
20. Crespo ÂC, Mulik S, Dotiwala F, Ansara JA, Sen Santara S, Ingersoll K, et al. Decidual NK cells transfer granulysin to selectively kill bacteria in trophoblasts. Cell 2020;182:1125–39.e18.
21. Guo C, Cai P, Jin L, Sha Q, Yu Q, Zhang W, et al. Single-cell profiling of the human decidual immune microenvironment in patients with recurrent pregnancy loss. Cell Discov 2021;7:1.
22. Rhinn M, Ritschka B, Keyes WM. Cellular senescence in development, regeneration and disease. Development 2019;146:dev151837.
23. Velicky P, Meinhardt G, Plessl K, Vondra S, Weiss T, Haslinger P, et al. Genome amplification and cellular senescence are hallmarks of human placenta development. PLoS Genet 2018;14:e1007698.
24. Kong C, Ordoñez AA, Turner S, Tremaine T, Muter J, Lucas ES, et al. Embryo biosensing by uterine natural killer cells determines endometrial fate decisions at implantation. FASEB J 2021;35:e21336.
25. Lei D, Zhang XY, Zheng PS. Recurrent pregnancy loss: fewer chromosomal abnormalities in products of conception? a meta-analysis. J Assist Reprod Genet 2022;39:559–72.
26. Hassold T, Hall H, Hunt P. The origin of human aneuploidy: where we have been, where we are going. Hum Mol Genet 2007;16:R203–8.
27. Jena MK, Nayak N, Chen K, Nayak NR. Role of macrophages in pregnancy and related complications. Arch Immunol Ther Exp (Warsz) 2019;67:295–309.
28. Yang HL, Lai ZZ, Shi JW, Zhou WJ, Mei J, Ye JF, et al. A defective lysophosphatidic acid-autophagy axis increases miscarriage risk by restricting decidual macrophage residence. Autophagy 2022;18:2459–80.
29. Guo YE, Li Y, Cai B, He Q, Chen G, Wang M, et al. Phenotyping of immune and endometrial epithelial cells in endometrial carcinomas revealed by single-cell RNA sequencing. Aging (Albany, NY) 2021;13:6565–91.
30. Garcia-Alonso L, Handfield LF, Roberts K, Nikolakopoulou K, Fernando RC, Gardner L, et al. Mapping the temporal and spatial dynamics of the human endometrium in vivo and in vitro. Nat Genet 2021;53:1698–711.
31. Gellersen B, Brosens JJ. Cyclic decidualization of the human endometrium in reproductive health and failure. Endocr Rev 2014;35:851–905.

Perfil de célula única del microambiente en tejido decidual de mujeres con aborto diferido.

Objetivo: Definir el microambiente decidual en abortos diferidos euploides y aneuploides y en interrupción voluntaria de gestaciones.

Diseño: Estudio prospectivo, multicéntrico y observacional.

Lugar: Hospital terciario y análisis descriptivo de datos transcriptómicos.

Pacientes: Un total de 34 pacientes experimentaron abortos, incluyendo 6 mujeres sometidas a interrupción voluntaria del embarazo de gestaciones no planificadas y 28 casos de abortos diferidos. Todas las pacientes realizaron sus operaciones de Sept 2021 a Sept 2022.

Intervenciones: Todas las mujeres se sometieron a la secuenciación de la variación del número de copias de las vellosidades. Mientras tanto, la secuenciación del RNA de célula única fue realizada en tejido decidual de 16 mujeres, y la retrotranscripción y reacción en cadena de la polimerasa cuantitativa se realizó en tejido decidual de 18 mujeres.

Variable principal: La secuenciación del ARN de célula única se utilizó para explorar los cambios en el microambiente de los tejidos deciduales de abortos.

Resultados: La secuenciación del ARN de célula única indicó que el microambiente del tejido decidual del grupo aborto diferido estaba alterada, y que las células estromales (SC), células natural killer y las células epiteliales reflejaban todas alteraciones funcionales en comparación con el grupo de interrupción voluntaria del embarazo. Se observó además una correlación entre la proporción de SC senescentes y las anormalidades cromosómicas en embriones de aborto diferido. La proporción de SC deciduales senescentes en el tejido decidual de las pacientes con aborto diferido con anormalidades cromosómicas comunes del feto era mayor, y esto no era favorable para el crecimiento fetal y estaba íntimamente relacionado con el aborto diferido. Además, comprobamos que la potencia de la interacción HLA-KIR entre los subgrupos NK1 y NK2 y los subtipos de células estromales no senescentes en los tejidos deciduales del aborto diferido era débil, jugando potencialmente un papel en la ocurrencia del aborto diferido.

Conclusión: La decidualización de las SC en tejidos deciduales de abortos diferidos estaba alterada, la eliminación de las células SC senescentes por las células NK disminuida, la toxicidad letal de las SC no senescentes aumentada, los macrófagos no residían de forma insuficiente en la interfase materno-fetal, y la diferenciación de células epiteliales estaba desequilibrada- creando todo un microambiente materno que no era propicio para el crecimiento fetal. Proponemos que interferir con la expresión de genes alterados en los tejidos deciduales del aborto diferido y revertir el microambiente materno podría constituir un medio eficaz para mejorar el resultado clínico de los abortos diferidos. Curiosamente, observamos una correlación entre la senescencia de las células del estroma y las anomalías cromosómicas embrionarias. Por tanto, hipotetizamos que el marcador de células SC senescentes DI02 puede ser utilizado como un marcador de riesgo en la incidencia de los abortos diferidos con anormalidades cromosómicas del embrión, y que puede ser aplicado para guiar el diagnóstico clínico y el tratamiento del aborto recurrente.